

Nonablative laser treatment of facial rhytides

Gary Lask^a, Patrick K. Lee^a, Manouchehr Seyfzadeh^a,
J. Stuart Nelson^b, Thomas E. Milner^b, Bahman Anvari^{b,c}, Digant Dave^b,
Roy G. Geronemus^d, Leonard J. Bernstein^d, Harry Mittelman^e, Laurie A. Ridener^f, Walter F. Coulson^g,
Bruce Sand^h, Jon Baumgardner^h, David Henningsⁱ, Richard Menefeeⁱ, and Michael Berryⁱ

^aUCLA Dermatology Laser Surgery Center, 200 Medical Plaza, Los Angeles, CA 90024

^bBeckman Laser Institute and Medical Clinic, University of California, Irvine, CA 92715

^cHarvey Mudd College, Department of Engineering, Claremont CA 91711 (Present Address)

^dLaser and Skin Surgery Center of New York, 317 East 34th Street, New York, NY 10016

^e2200 Sand Hill Road, Menlo Park, CA 94025 ^fBuckman Company, Concord, CA 94520

^gUCLA Center for Health Sciences, Department of Pathology, Los Angeles, CA 90095

^hLaser Aesthetics, Inc., 8383 Wilshire Boulevard, Suite 440, Beverly Hills, CA 90211

ⁱNew Star Lasers, Inc., 11802 Kemper Road, Auburn, CA 95603

ABSTRACT

The purpose of this study is to evaluate the safety and effectiveness of the New Star Model 130 neodymium:yttrium aluminum garnet (Nd:YAG) laser system for nonablative laser treatment of facial rhytides (*e.g.*, periorbital wrinkles). Facial rhytides are treated with 1.32 μm wavelength laser light delivered through a fiberoptic handpiece into a 5 mm diameter spot using three 300 μs duration pulses at 100 Hz pulse repetition frequency and pulse radiant exposures extending up to 12 J/cm². Dynamic cooling is used to cool the epidermis selectively prior to laser treatment; animal histology experiments confirm that dynamic cooling combined with nonablative laser heating protects the epidermis and selectively injures the dermis. In the human clinical study, immediately post-treatment, treated sites exhibit mild erythema and, in a few cases, edema or small blisters. There are no long-term complications such as marked dyspigmentation and persistent erythema that are commonly observed following ablative laser skin resurfacing. Preliminary results indicate that the severity of facial rhytides has been reduced, but long-term follow-up examinations are needed to quantify the reduction. The mechanism of action of this nonablative laser treatment modality may involve dermal wound healing that leads to long-term synthesis of new collagen and extracellular matrix material.

BACKGROUND

Facial rhytides (*e.g.*, periorbital and perioral wrinkles produced by photodamage and/or aging) have previously been treated using a variety of modalities, including dermabrasion, chemabrasion (chemical peel), and CO₂ laser skin resurfacing (LSR) - a technique in which pulsed or scanned CO₂ laser light at 10.6 μm wavelength is used to ablate skin. All three modalities provoke a strong skin wound healing response that leads to wrinkle reduction. CO₂ LSR has recently emerged as a widely used aesthetic surgical modality which may have advantages of improved reproducibility and control compared to dermabrasion and chemabrasion^[1-10]. However, CO₂ LSR is often accompanied by complications such as persistent erythema, hyperpigmentation, hypopigmentation, scarring, and infection^[1-10]. Patients also experience edema, drainage, and burning discomfort during, typically, the first few weeks after treatment. The work reported in this paper is directed toward treating facial rhytides using a new nonablative laser modality that may be effective in reducing both the severity of wrinkles and the incidence of morbidity presently associated with LSR.

The mechanism of action of CO₂ LSR is not well understood, but three processes have been identified as possible contributors to facial rhytides reduction^[1]: 1) ablation of the epidermis and part of the dermis, 2) acute collagen shrinkage in the residual dermis, and 3) long-term wound healing that leads to dermal remodelling as new collagen and extracellular matrix material are synthesized over a period of months after treatment. Dermal ablation may be useful to remove dermal surface irregularities such as acne scars^[11], but may not be a major contributor to rhytides reduction. Dermal collagen shrinkage induced by CO₂ LSR has been studied by *in vivo* pig skin experiments^[12] and *in vitro* human skin experiments^[13]; this process may contribute to acute wound contraction, but may be only incidental to long-term rhytides reduction. Long-term wound healing and dermal remodelling is probably the major mechanism of action responsible for long-term facial rhytides reduction; clinical evidence for this hypothesis includes the following studies.

In one ablative LSR clinical study^[5], a pulsed CO₂ LSR device was used to treat periorbital and/or perioral rhytides of 100 patients; reduction in the severity of facial rhytides was quantitated by grading of pre- and post-treatment photographs using a visual analog scale (0=no improvement, ..., 6=marked improvement). At 1 month post-treatment, only 5 of 100 patients exhibited marked improvement, while 68 and 27 patients exhibited moderate or minimal improvement, respectively. At 2 months post-treatment, 20 of 27 patients with minimal improvement at 1 month exhibited further (moderate to marked) improvement from baseline. Mean (\pm standard deviation) improvement grades increased from 2.30 ± 1.18 (n=100 cases) at 1 month to 3.07 ± 0.99 (n=83) at 2 months, 3.74 ± 1.04 (n=87) at 3 months, and 4.17 ± 1.18 (n=38) at 6 months post-treatment. Since significant cumulative reduction of facial rhytides occurred from 1 month to 6 months after CO₂ LSR treatment, long-term wound healing must have been a major component of the mechanism of action.

Long-term wound healing, including dermal collagen synthesis, has been documented as an important mechanism of action for both dermabrasion^[14-15] and chemabrasion^[16] reduction of wrinkles in photodamaged skin. For example, in one dermabrasion clinical study^[14], a rotating diamond fraise dermabrasion device was used to treat photodamaged facial skin of 10 patients; the clinical severity of photodamage was quantitated by grading of pre- and 12 week post-treatment photographs using a photonumeric scale (0=no wrinkles or other photodamage, 1 through 3=mild, 4 through 6=moderate, 7 through 9=severe). Wrinkle severity decreased from a mean (\pm standard error) pre-treatment value of 4.9 ± 0.5 to 3.7 ± 0.5 at 12 weeks post- ($p=0.016$; paired t-test). Histologic grading using Masson trichrome stain showed that mean collagen density in the upper dermal repair zone increased from 0.8 ± 0.2 pre-treatment to 1.7 ± 0.3 at 3 weeks and 2.6 ± 0.5 at 12 weeks post- ($p=0.004$ and 0.007 ; paired t-tests); there were no other significant histologic changes (*e.g.*, in elastin density or epidermal thickness). *In situ* hybridization analysis for fibroblast procollagen I mRNA showed that wrinkle severity reduction for individual patients at 12 weeks post-treatment correlated strongly with patient increases in fibroblast procollagen I mRNA from baseline. Both immunohistologic staining and immunoblotting showed that papillary dermal fibroblast synthesis of procollagen I increased substantially (3 to 4.2 times baseline at 3 weeks post- and 1.5 to 2.7 times baseline at 12 weeks post-treatment). These studies conclude that papillary dermal fibroblasts are activated to synthesize procollagen I (the synthetic precursor to collagen I, the most abundant dermal protein) during long-term wound healing response to superficial dermal injury. Histologic studies on CO₂ LSR^[17-18] have identified similarities in wound healing and collagen synthesis in comparison to dermabrasion and chemabrasion, so all three modalities are likely to have the same mechanism of action.

Ablation or other means of removing the epidermis are not necessary to provoke dermal wound healing response. Topical applications of tretinoin (all-*trans*-retinoic acid)^[19] and α -hydroxy acids (*e.g.*, glycolic acid)^[20] lead to reduced wrinkles and increased papillary dermal collagen I. It is also notable that a pulsed 1.06 μ m wavelength Nd:YAG laser has been used successfully in some cases to treat facial rhytides without ablation^[21].

METHODOLOGY OF NONABLATIVE LASER TREATMENT

The present nonablative laser treatment procedure is designed to produce selective papillary dermal injury leading to fibroblast activation and synthesis of new collagen and extracellular matrix material without significant epidermal injury. Two requirements must be satisfied to achieve this favorable treatment:

- 1) the laser wavelength, waveform, and radiant exposure must be selected to damage the papillary dermis and activate fibroblasts, thereby yielding a long-term wound healing response, and
- 2) the epidermis must be protected by, for example, cooling prior to laser exposure.

The laser selected for the procedure is a New Star (NS) Model 130 neodymium:yttrium aluminum garnet (Nd:YAG) device operating at 1.32 μm laser wavelength with a pulse waveform of three nearly-identical 300 μs duration pulses delivered at 100 Hz pulse repetition frequency (yielding a 20 ms duration macropulse containing three micropulses). The laser output is delivered through an optical fiber and focussing lens combination to produce a 5 mm diameter spot on the stratum corneum. The laser pulse energy is adjustable to yield pulse radiant exposures (*i.e.*, pulse areal energy densities) up to 15 J/cm^2 . Since the three micropulses are delivered within 20 ms, a relatively fast time for which the mean thermal diffusion length is *ca.* 10 μm ^[22], the three micropulses produce tissue effects that are nearly the same as those produced by one macropulse of 20 ms duration with 3 times the micropulse radiant exposure. In discussion below, the 3-pulse (or macropulse) radiant exposure will be used and termed simply the “radiant exposure”.

In contrast to ablative lasers (*e.g.*, CO_2 and Er:YAG lasers which produce wavelengths of light that are absorbed within a few tens of microns of both native and partly dehydrated tissue surfaces), the NSL Model 130 laser wavelength of 1.32 μm produces in depth optical heating of, and thermal damage to, the papillary dermis and superficial reticular dermis (within a zone *ca.* 100 μm thick located just below the epidermis, which is *ca.* 50 to 100 μm thick in periorbital skin; see Animal Histology Experiments section below). At 1.32 μm wavelength, the primary tissue chromophore is water, which has an absorption coefficient of 1.82 cm^{-1} ^[23]. Assuming that the mean water concentration in the epidermis and papillary dermis is 70% by weight^[24] and that skin density is 1.1 g/cm^3 ^[25], the skin absorption coefficient μ_a is *ca.* 1.4 cm^{-1} , corresponding to an optical absorption depth δ_a ($= 1/\mu_a$) of *ca.* 0.71 cm. Scattering of 1.32 μm wavelength light by skin microstructures (*e.g.*, collagen fibers) markedly changes the distribution of laser light from an exponential attenuation of the incident radiant exposure F_0 [$F(z=0)$, neglecting reflection at the air/tissue interface] as a function of tissue depth z (units: cm):

$$F(z) = F_0 \exp(-\mu_a z) = F_0 \exp(-z/\delta_a) \quad (1)$$

to a more complex distribution [which can be calculated by Monte Carlo modelling^[26] if the scattering properties (*e.g.*, the scattering coefficient μ_s and the anisotropy factor g) are known]. Figure 1 shows the difference between light distributions for model “absorption only (A: $\mu_a = 1 \text{ cm}^{-1}$, $\mu_s = 0$)” and “absorption plus scattering (A+S: $\mu_a = 1 \text{ cm}^{-1}$, $\mu_s = 100 \text{ cm}^{-1}$, $g = 0.9$)^[26]” cases. The fluence $\phi(z)$ [units: J/cm^2] is the photon energy from all directions (including backscattered light within the tissue) passing through a unit area located at depth z ; the corresponding radiant exposure $F(z)$ is the photon energy from the original direction of light propagation (in the absence of scattering) passing through the same unit area. For “absorption only”, $\phi(z) = F(z)$; for “absorption plus scattering”, backscattering increases the fluence [*i.e.*, $\phi(z) > F(z)$] near the air/tissue interface and decreases the fluence [*i.e.*, $\phi(z) < F(z)$] deep within the tissue. For “absorption only”, the 1.32 μm wavelength photon energy reflected from the air/tissue interface is a small percentage (*ca.* 2%) of the incident photon energy, while for “absorption plus scattering”, the 1.32 μm wavelength photon energy remitted from the tissue can be a larger percentage due to both direct reflection and backscattered transmission contributions^[27-28].

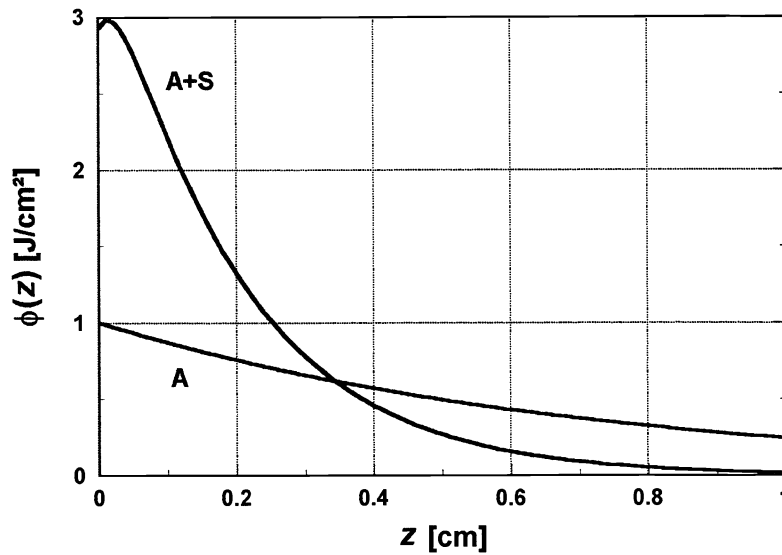


Figure 1: 1.32 μm relative light distributions ($F_0 = 1 \text{ J/cm}^2$) for absorption only (A: $\mu_a = 1 \text{ cm}^{-1}$, $\mu_s = 0$) and for absorption plus scattering^[26] (A+S: $\mu_a = 1 \text{ cm}^{-1}$, $\mu_s = 100 \text{ cm}^{-1}$, $g = 0.9$; air/tissue interface)

The “absorption plus scattering” light distribution function (A+S in Figure 1) is expected to be similar to that obtained in human skin (although the scattering coefficient μ_s is probably a function of the amount of photodamage, the chronological age, and other patient-dependent factors). Light absorption and temperature increase are proportional to the light distribution function; although distribution function A+S exhibits a subsurface peak, thermal damage in the epidermis will be nearly the same as that in the papillary dermis if only laser treatment is performed. Instead, “dynamic cooling”^[29-32] is used to protect the epidermis; this technique involves selectively cooling the epidermis by delivering a spurt of cryogen for a period of tens of milliseconds onto the stratum corneum immediately before laser treatment. Figure 2 shows schematic temperature increases *vs.* tissue depth for “laser only” (L) and “dynamic cooling plus laser” (C+L) treatments, using the “absorption plus scattering” light distribution (A+S in Figure 1) with a radiant exposure of 30 J/cm^2 for both cases. Case C+L in Figure 2 includes initial cooling with a cryogen spurt of 20 ms duration followed by 5 ms delay before laser irradiation. Temperature increases between 30 to 40 °C above physiological temperature applied over a period of several ms cause phase transition of collagen I within the papillary dermis and superficial reticular dermis^[33]; this collagen thermal modification is probably sufficient to activate fibroblasts to produce long-term wound healing response. If this temperature-time history is effective, temperature increase function C+L in Figure 2 may be nearly ideal to produce selective thermal damage in the superficial dermis while protecting the epidermis from injury. “Fine-tuning” of nonablative laser treatments can be obtained by controlling three parameters: 1) dynamic cooling (cryogen type and application time), 2) temporal delay (between the cryogen cooling pulse and the laser heating pulse), and 3) laser heating (radiant exposure, as well as wavelength and waveform in other lasers). Histology experiments that demonstrate the effects of nonablative laser treatment parameters are discussed below.

Further basic science aspects of nonablative laser treatment [including pulsed photothermal radiometry (PPTR) measurements of skin front surface temperatures produced by nonablative laser irradiation and optical/thermal modelling of light, temperature increase, and damage distributions in laser-irradiated skin] are presented in a companion paper^[34].

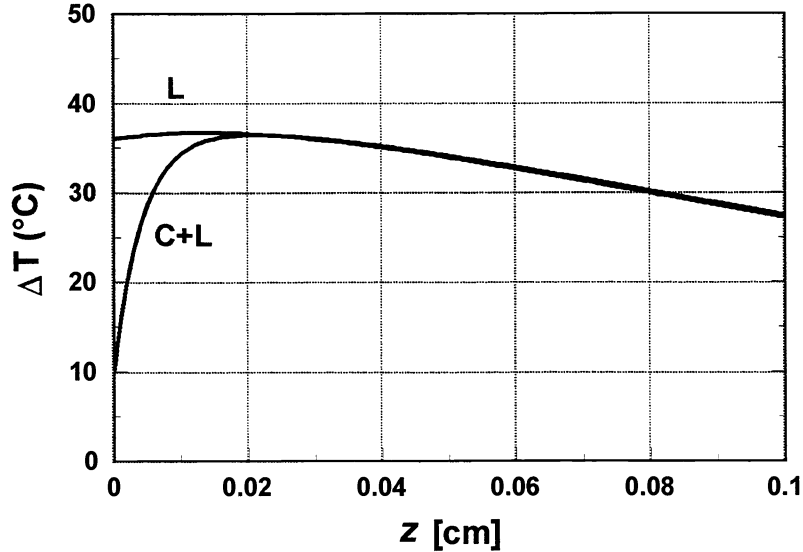


Figure 2: Temperature increase distributions for laser only (L: $F_0 = 30 \text{ J/cm}^2$) and for dynamic cooling plus laser (C+L: $F_0 = 30 \text{ J/cm}^2$ delivered after a 20 ms cryogen spurt and 5 ms delay)

ANIMAL HISTOLOGY EXPERIMENTS

A porcine skin model was used to evaluate near-acute effects of nonablative laser treatments over a range of dynamic cooling and laser heating conditions. A grid of 5.2 X 3.4 cm treatment and control sites was marked in permanent black ink on the abdomen of an anaesthetized 3-month old, 25-kg female Yorkshire pig. Treatment sites were irradiated through 6 mm diameter hole patterns in adhesive-backed templates mounted on each site; a series of 9 templates, each of which provided a different hole pattern, was used to produce a nearly-uniform treatment (totalling 171 macropulses) within each site. Cryogen spurts and laser light pulses were delivered using a handpiece equipped with a transparent plastic barrel and red HeNe laser aiming beam to facilitate delivery centration and to produce a fixed spot size and irradiance distribution within each template hole. Laser radiant exposures were calculated using measurements of macropulse energies delivered through a 3.18 mm diameter aperture centered in the beam; although the laser spot size is nominally as large as 5 mm, the laser irradiance distribution is peaked centrally so that most of the tissue effects occur within the central 3 mm diameter of each spot. Four laser heating radiant exposures (26, 30, 36, and 39 J/cm^2) were delivered to treatment sites that were uncooled (*i.e.*, at physiological temperature) or that were pre-cooled with either 20 ms or 40 ms durations of cryogen spurts; when cryogen pre-cooling was used, the laser heating macropulse started after a 5 ms delay following the completion of the cryogen spurt. Other sites were treated with coolant only (20 and 40 ms duration cryogen spurts) or were used as controls.

Full-thickness 4-mm diameter punch biopsy specimens were obtained from treatment and control sites 2 days after treatment. Specimens were fixed in 10% formalin, dehydrated in graded ethanol solutions and xylene, embedded in paraffin, cut into 4 μm thick sections, and prepared for standard and polarized light microscopy examinations using hematoxylin-eosin (HE), Masson's trichrome (M) for collagen, and Verhoeff-van Gieson (VvG) for elastin stains. Figure 3 shows photomicrographs of control and treated ($F = 30 \text{ J/cm}^2$) specimens.

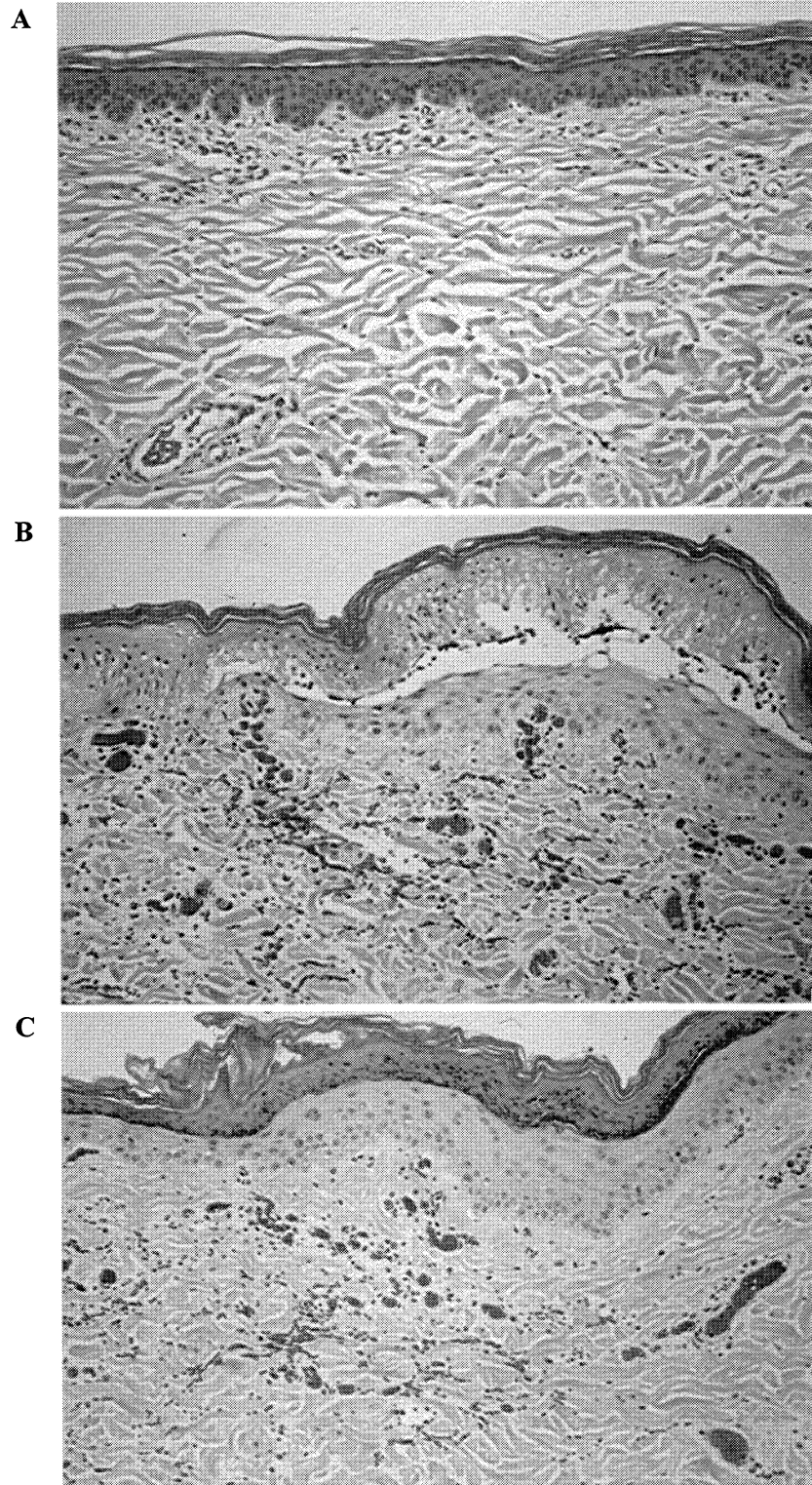


Figure 3: (All with HE stain) **A** - Control, X4 objective; **B** - $F = 30 \text{ J/cm}^2$, no coolant, X10 objective; **C** - same as **B**, but with 20 ms coolant prior to laser

Figure 3A (control - no coolant or laser) shows normal skin (total thickness shown: *ca.* 1.2 mm) comprising epidermis (E) on top (*ca.* 75 to 150 μm thickness in various locations), followed by the papillary dermis (PD) layer (*ca.* 50 to 75 μm additional thickness), and a portion of the reticular dermis (RD) layer. Figure 3B shows treated skin (laser only: $F = 30 \text{ J/cm}^2$; total thickness shown: *ca.* 450 μm) displaying massive damage to E with a large blister plus significant damage to the PD and superficial RD layers. Figure 3C shows treated skin (same as 3B, but with 20 ms coolant) with little or no E necrosis, but substantial PD and superficial RD injury. Additional specimens (not shown; same as 3C, but with M stain) show some collagen fiber modification by subtle changes in stain coloration. Using polarized light, these specimens show loss of collagen birefringence in the PD and superficial RD layers. Loss of collagen birefringence is uniquely associated with thermal damage^[35], which becomes appreciable (*i.e.*, damage integral $\Omega \geq 1$ ^[36]) in skin heated at temperatures above *ca.* 70 °C for a timescale of tens of ms (corresponding to the approximate cooldown time following heating by the laser macropulse). This is just the condition that may activate fibroblasts and stimulate long-term wound healing response, including new collagen synthesis and subsequent reduction in wrinkle severity.

Promising near-acute histology effects (*i.e.*, significant thermal damage to the superficial dermis with little or no epidermal damage) were also observed for $F = 26 \text{ J/cm}^2$ with 20 ms coolant, $F = 30 \text{ J/cm}^2$ with 40 ms coolant, and for $F = 36 \text{ J/cm}^2$ with 40 ms coolant. Coolant durations of 20 ms or less did not prevent E necrosis at the highest radiant exposures ($F = 36$ and 39 J/cm^2) and even 40 ms pre-cooling did not prevent E necrosis at $F = 39 \text{ J/cm}^2$. At $F = 36$ and 39 J/cm^2 , skin shrinkage was observed immediately following laser irradiation. Interestingly, prompt skin/collagen shrinkage generated wrinkles in the previous unwrinkled pig abdomen skin.

Future animal histology experiments will include refinement of treatment conditions (including higher resolution variations of cooling, delay, and heating parameters), together with longer term (*i.e.*, at least 3 months post-treatment) follow-up measurements by standard light, polarized light, and transmission electron microscopy. Immunohistochemical stains will also be used to identify procollagen I and other synthetic products of activated fibroblasts and to correlate long-term wound healing response to short-term thermal injury. Observed tissue effects will also be correlated with measured skin surface temperature increases.

HUMAN CLINICAL STUDY

A human clinical study is being performed to evaluate the safety and effectiveness of the New Star (NSL) Model 130 Nd:YAG laser system for nonablative laser treatment of facial rhytides. To date, twenty (of a planned total of sixty-five) patients have been treated in an outpatient setting at three sites. The study had been approved by the Institutional Review Board of each site before commencement of treatments.

Twenty patients [18 women, 2 men; mean age (\pm standard deviation): 48.5 ± 7.0 years; range: 40 to 68 years] with photodamaged skin were treated in both right and left periorbital skin areas to reduce rhytides. All patients were Caucasian, with sun-reactive skin types I ($n=10$ cases) and II ($n=10$ cases)^[37]. Classification of wrinkle severity was performed prior to treatment as Class I (fine wrinkles; $n=4$), Class II (fine to moderate-depth wrinkles, moderate number of lines; $n=14$), or Class III (fine to deep wrinkles, numerous lines, with or without redundant skin folds; $n=2$)^[8]. Pre-treatment inclusion criteria included Caucasian race, sun-reactive skin types I or II, age between 40 and 70 years, photodamaged skin of Classes I through III with periorbital and/or perioral rhytides covering an area of at least one cm^2 , ability to read, understand, and sign an Informed Consent form, and ability and willingness to comply with all follow-up requirements. Pre-treatment exclusion criteria included active localized or systemic infections, immunocompromised status, coagulation disorders, photosensitivity or allergy, use of aspirin or antioxidants, mental incompetence, pregnancy, and prisoner status.

Pre-treatment examinations included standardized photography and standardized silicone replicas for optical profilometry measurements. Silicone replicas were obtained by trained personnel using silicone rubber impression material and catalyst (Silflo, Flexico Developments Ltd., Potters Bar, England) using methods similar to those previously described^[38]. Periorbital areas were anaesthetized with EMLA cream (a eutectic mixture of local anaesthetics - 2.5% lidocaine and 2.5% prilocaine plus 92% water and 3% emulsifiers and thickening agent; Astra USA, Westborough, MA) applied at least 45 minutes before treatment. Rectangular treatment sites (5.2 cm long X 3.4 cm wide) were centered on periorbital areas and treatments were completed through a series of template holes as described above (see Animal Histology Experiments section). The mean treatment radiant exposure was 24.7 ± 0.6 J/cm² (range: 23 to 25 J/cm²); laser energy was delivered following a 40 ms coolant spurt and subsequent 5 ms delay. The coolant also provided a local anaesthetic effect (combined with that of the EMLA cream) so that patients typically felt little pain; on a 0 to 4 point pain assessment scale (0=no, 1=mild, 2=moderate, 3=severe, 4=intolerable), the mean patient subjective pain was 1.2 ± 1.1 and 1.5 ± 1.0 on the right and left sides of the face, respectively. It is believed that patients who felt "severe" pain (n=1 case) or "intolerable" pain (n=2 cases) in one or both treatment sites received inadequate EMLA anaesthetic; in future treatments, EMLA will be applied for at least 1.5 hours prior to treatment and, in fact, even longer application times would be more effective^[39]. Patient pain in one case may also have been due to inadequate cooling. Treatments were interrupted by a technical problem (fiber breakage) in one case and by pain in another case.

Immediately post-treatment, all patients had some degree of erythema in treated sites; additionally, two patients had edema and one had small blisters. Three patients (all treated on the same morning at one site) developed swelling at their left (but not right) periorbital treatment sites the evening of the treatment day; these sites blistered and drained clear fluid on the next morning, leaving superficial erosions. These injuries, which are believed to be due to fiber damage that led to excess cryogen cooling, resolved after wound care and Polysporin application; the delivery handpiece was subsequently redesigned to prevent optical fiber tip contamination and damage. Most of the treated site blemishes disappeared within 7 days, but at 1 month post-treatment, 3 of the 19 patients examined (16% incidence) had minor blemishes (one small bump, one very slight hyperpigmentation, and one hyperpigmentation).

Post-treatment examinations (including assessments of improvement and outcome, clinical observations, and, with reduced frequency, standardized photography and silicone replica impressions) are being obtained at 1 day, 1 week, 1 month, 3 months, and 6 months after treatment. At present, the follow-up statistics are: n=8 (40%) at 1 day, n=16 (80%) at 1 week, n=19 (95%) at 1 month, and n=2 (10%) at 3 months post-treatment.

Wrinkle severity improvement (WSI) assessment (from baseline) was made subjectively by the treating physicians using four improvement grade levels: 1 (0-25%), 2 (26-50%), 3 (51-75%), and 4 (76-100%). Outcome assessment was graded subjectively by the treating physicians using four levels: 1 (poor), 2 (fair), 3 (good), and 4 (excellent). At 1 week post-treatment, WSI was graded 1 in all cases, but outcome assessment was graded 1 in 6 cases (38% incidence) and 2 in the other 10 cases (63% incidence). At 1 month post-treatment, WSI was graded 1 in 13 cases (72%) but was graded 2 in 5 cases (28%), while outcome assessment also improved to a grade of 1 in 4 cases (22%) and 2 in 14 cases (78%). Anecdotally, at 1 month after treatment, most patients subjectively believe that their wrinkle severity has been reduced from baseline. Photographic and profilometric data are being obtained to provide more objective assessments of wrinkle reduction and overall outcome.

At this early stage of the human clinical study, all the patients have received low radiant exposure treatments (below the apparent damage threshold in pig histology experiments). These conservative treatments were performed, in part, to learn whether sub- or near-threshold injury is sufficient to activate fibroblasts to

synthesize new collagen and other extracellular matrix materials. Indeed, there are numerous claims of “biostimulation” of fibroblast activation and wound healing improvement using relatively low power lasers^[40], so testing the possible effectiveness of low radiant exposure treatments is desirable. At present, with relatively short-term follow-up, our clinical results indicate that mild wrinkle reduction may be obtained at low radiant exposure levels in some cases. Longer-term follow-up will provide proper outcome assessment, but in the meantime additional patients will be treated at higher laser radiant exposures (and/or at shorter coolant durations) to achieve more effective periorbital wrinkle reductions.

CONCLUSIONS AND FUTURE STUDIES

The development of this nonablative laser treatment procedure is at an early stage. It is still necessary to find the “narrow therapeutic window” of cryogen cooling and laser heating treatment parameters through which effective treatments can be obtained routinely. These effective treatment parameters will be determined through further animal histology and human clinical studies

A new diagnostic device is also being developed to provide improved and patient- and/or site-specific treatments. This diagnostic device includes a radiometer mounted in the delivery handpiece that permits real-time temperature measurements of the skin surface at the treatment site. The device will be used to verify that cryogen application has pre-cooled each site prior to laser light delivery; a feedback signal from the device will then enable laser operation. More importantly, the radiometer will measure the skin front surface temperature rise following irradiation at a diagnostic (*i.e.*, well below therapeutic threshold) radiant exposure level; this information will then be used to calibrate the correct radiant exposure that must be delivered to achieve the papillary dermis temperature increase required to activate fibroblasts and to stimulate their long-term wound healing response. The clinical value of this diagnostic device is that it will facilitate adjustment of laser light delivery to overcome variations in skin optical properties, which are highly patient-specific. For example, the absorption coefficient of skin at 1.32 μm depends strongly on skin hydration, which varies with age and other factors. In addition, the scattering properties of skin at 1.32 μm are likely to depend strongly upon the amount of photodamage, chronological age, skin type, and other factors; the right and left periorbital sites may even be asymmetrically photodamaged^[41], requiring treatment optimizations to reduce rhytides.

It is anticipated that future refinements of this nonablative laser treatment device and procedure will permit safe and effective treatments of facial rhytides for most patients. Complications should be low or nonexistent when the “narrow therapeutic window” of proper cryogen cooling and laser heating treatment parameters is used. In addition, the current approach should permit effective treatments of patients with pigmented skin who have thusfar been difficult to treat successfully by CO₂ LSR (due to the high risk of dyspigmentation). Since melanin is located in the epidermis^[27] which is protected by dynamic cooling, and since melanin does not absorb 1.32 μm wavelength light, the current nonablative laser treatment will probably not cause substantial dyspigmentation. Clinical verification of this application will be pursued.

ACKNOWLEDGEMENTS

This work was sponsored, in part, by the National Institutes of Health (on Grants 1R29 AR41638-01A1, 1R01 AR42437-01A1, and 1R01 AR4341901A1), the National Science Foundation (on Grant BES-9634110), and the Whitaker Foundation (on Grant WF 21025). The authors thank the sponsoring organizations and also thank Michael Brewer, Carol Appleton, Richard Gayek DVM, P. Timothy Lawson DVM, Silas Lacy, and Lonnie Bivens for technical and clinical contributions to this work.

REFERENCES

1. Hruza GJ. Laser skin resurfacing. *Arch Dermatol*. 1996;132:451-455.
2. Waldorf HA, Kauvar ANB, Geronemus RG. Skin resurfacing of fine to deep rhytides using a char-free carbon dioxide laser in 47 patients. *Dermatol Surg*. 1995;21:940-946.
3. Lowe NJ, Lask G, Griffin ME. Laser skin resurfacing: pre- and post-treatment guidelines. *Dermatol Surg*. 1995;21: 1017-1019.
4. Lask G, Keller G, Lowe N, Gormley D. Laser skin resurfacing with the SilkTouch flashscanner for facial rhytides. *Dermatol Surg*. 1995;21:1021-1024.
5. Lowe NJ, Lask G, Griffin ME, Maxwell A, Lowe P, Quilada F. Skin resurfacing with the Ultrapulse carbon dioxide laser: observations on 100 patients. *Dermatol Surg*. 1995;21:1025-1029.
6. David LM, Sarne AJ, Unger WP. Rapid laser scanning for facial resurfacing. *Dermatol Surg*. 1995;21:1031-1033.
7. Ho C, Nguyen Q, Lowe NJ, Griffin ME, Lask G. Laser resurfacing in pigmented skin. *Dermatol Surg*. 1995;21:1035-1037.
8. Fitzpatrick RE, Goldman MP, Satur NM, Tope WD. Pulsed carbon dioxide laser resurfacing of photoaged facial skin. *Arch Dermatol*. 1996;132:395-402.
9. Grevelink JM. Facial contouring using a flashscanner-enhanced carbon dioxide laser. *Facial Plastic Surg Clinics North Amer*. 1996;4:241-246.
10. Felder DS, Mayl N. Periorbital carbon dioxide laser resurfacing. *Seminars in Ophthalmol*. 1996;11:201-210.
11. Alster TS, West TB. Resurfacing of atrophic facial acne scars with a high-energy pulsed carbon dioxide laser. *Dermatol Surg*. 1996;22:151-155.
12. Ross EV, Naseef GS, Skrobal M, Grevelink JM, Anderson RR. *In vivo* dermal collagen shrinkage and remodeling following CO₂ laser resurfacing. *Lasers Surg Med*. 1996;Supplement 8:38.
13. Gardner ES, Reinisch L, Stricklin GP, Ellis DL. *In vitro* changes in non-facial human skin following CO₂ laser resurfacing: a comparison study. *Lasers Surg Med*. 1996;19:279-387.
14. Nelson BR, Majmudar G, Griffiths CE, Gillard MO, Dixon AE, Tavakkol A, Hamilton TA, Woodbury RA, Vorrhees JJ, Johnson TM. Clinical improvement following dermabrasion of photoaged skin correlates with synthesis of collagen I. *Arch Dermatol*. 1994;130:1136-1142.
15. Nelson BR, Metz RD, Majmudar G, Hamilton TA, Gillard MO, Railan D, Griffiths CEM, Johnson TM. A comparison of wire brush and diamond fraise superficial dermabrasion for photoaged skin: a clinical, immunohistologic, and biochemical study. *J Am Acad Dermatol*. 1996;34:235-243.
16. Nelson BR, Fader DJ, Gillard M, Majmudar G, Johnson TM. Pilot histologic and ultrastructural study of the effects of medium-depth chemical facial peels on dermal collagen in patients with actinically damaged skin. *J Am Acad Dermatol*. 1995;32:472-278.
17. Cotton J, Hood AF, Gonin R, Beeson WH, Hanke W. Histologic evaluation of preauricular and postauricular human skin after high-energy, short-pulse carbon dioxide laser. *Arch Dermatol*. 1996;132:425-428.

18. Fitzpatrick RE, Tope WD, Goldman MP, Satur NM. Pulsed carbon dioxide laser, trichloroacetic acid, Baker-Gordon phenol, and dermabrasion: a comparative clinical and histologic study of cutaneous resurfacing in a porcine model. *Arch Dermatol.* 1996;132:469-471.
19. Griffiths CEM, Russman AN, Majmudar G, Singer RS, Hamilton TA, Voorhees JJ. Restoration of collagen formation in photodamaged human skin by tretinoin (retinoic acid). *New Engl J Med.* 1993;329:530-535.
20. Ditre CM, Griffin TD, Murphy GF, Sueki H, Telegan B, Johnson WC, Yu RJ, Van Scott EJ. Effects of α -hydroxy acids on photoaged skin: a pilot clinical, histologic, and ultrastructural study. *J Am Acad Dermatol.* 1996;34:187-195.
21. Goldberg DJ. Evaluation of the Q-switched Nd:YAG laser for skin resurfacing. *Lasers Surg Med.* 1996; Supplement 8:35.
22. Valderrama GL, Fredin LG, Berry MJ, Dempsey BP, Harpole GM. Temperature distributions in laser-irradiated tissues. *SPIE Proc.* 1991;1427:200-213.
23. Kou L, Labrie D, Chylek P. Refractive indices of water and ice in the 0.65- to 2.5- μ m spectral range. *Appl Opt.* 1993;32:3531-3540.
24. von Zglinicki T, Lindberg M, Roomans GM, Forslind B. Water and ion distribution profiles in human skin. *Acta Derm Venereol (Stockh).* 1993;73:340-343.
25. Duck FA. *Physical Properties of Tissue: A Comprehensive Reference Book.* (Academic Press, London, 1990).
26. Jacques SL, Wang L. Monte Carlo modeling of light transport in tissues. In: Welch AJ, van Gemert MJC (editors). *Optical-Thermal Response of Laser-Irradiated Tissue.* (Plenum Press, New York, 1995), pp. 73-100.
27. Anderson RR, Parrish JA. Optical properties of human skin. In: Regan JD, Parrish JA (editors). *The Science of Photomedicine.* (Plenum Press, New York, 1982), pp. 147-194.
28. Welch AJ, van Gemert MJC, Star WM, Wilson BC. Definitions and overview of tissue optics. In: Welch AJ, van Gemert MJC (editors). *Optical-Thermal Response of Laser-Irradiated Tissue.* (Plenum Press, New York, 1995), pp. 15-46.
29. Anvari B, Milner TE, Tanenbaum BS, Kimel S, Svaasand LO, Nelson JS. Selective cooling of biological tissues: application for thermally mediated therapeutic procedures. *Phys Med Biol.* 1995;40:241-252.
30. Nelson JS, Milner TE, Anvari B, Tanenbaum BS, Kimel S, Svaasand LO. Dynamic epidermal cooling during pulsed laser treatment of port wine stain - a new methodology with preliminary clinical evaluation. *Arch Dermatol.* 1995;131:695-700.
31. Anvari B, Tanenbaum BS, Milner TE, Kimel S, Svaasand LO, Nelson JS. A theoretical study of the thermal response of skin to cryogen spray cooling and pulsed laser irradiation: implications for the treatment of port wine stain birthmarks. *Phys Med Biol.* 1995;40:1451-1465.
32. Nelson JS, Milner TE, Anvari B, Tanenbaum BS, Svaasand LO, Kimel S. Dynamic epidermal cooling in conjunction with laser-induced photothermolysis of port wine stain blood vessels. *Lasers Surg Med.* 1996;19:224-229.
33. Stringer H, Parr J. Shrinkage temperature of eye collagen. *Nature.* 1964;204:1307.
34. Milner TE, Anvari B, Smithies DJ, Dave D, Berry M, Hennings DR, Baumgardner J, Nelson J. Analysis of nonablative skin resurfacing. *SPIE Proc.* 1997;2970:xxx.

35. Thomsen S, Pearce JA, Cheong W-F. Changes in birefringence as markers for thermal damage in tissues. *IEEE Trans Biomed Engin.* 1989;36:1174-1179.
36. Pearce J, Thomsen S. Rate process analysis of thermal damage. In: Welch AJ, van Gemert MJC (editors). *Optical-Thermal Response of Laser-Irradiated Tissue.* (Plenum Press, New York, 1995), pp. 561-606.
37. Fitzpatrick TB. The validity and practicality of sun-reactive skin types I through VI. *Arch Dermatol.* 1988;124:869-871.
38. Grove GL, Grove MJ, Leyden JJ, Lufrano L, Schwab B, Perry BH, Thorne EG. Skin replica analysis of photodamaged skin after therapy with tretinoin emollient cream. *J Am Acad Dermatol.* 1991;25:231-237.
39. Gupta AK, Sibbald RG. Eutectic lidocaine/prilocaine 5% cream and patch may provide satisfactory analgesia for excisional biopsy or curettage with electrosurgery of cutaneous lesions. *J Am Acad Dermatol.* 1996;35:419-423.
40. Wheeland RG. Lasers for the stimulation or inhibition of wound healing. *J Dermatol Surg Oncol.* 1993; 19: 747-752.
41. Singer RS, Hamilton TA, Voorhees JJ, Griffiths CEM. Association of asymmetrical facial photodamage with automobile driving. *Arch Dermatol.* 1994;130:121-123. Erratum: *Arch Dermatol.* 1995;131:62.